Mühendislik Bilimleri ve Tasarım Dergisi
13(1), 202-220, 2025
e-ISSN: 1308-6693

Journal of Engineering Sciences and Design
DOI: 10.21923/jesd.1452157

Araştırma Makalesi Research Article

REVISITING BODE'S IDEAL LOOPS: INTEGRAL SQUARE ERROR OPTIMALITY OF BODE'S IDEAL LOOPS AND BODE'S IDEAL LOOP INVERSE CONTROLLER DESIGN

Barış Baykant ALAGÖZ[1], Furkan Nur DENİZ[2], Cemal KELEŞ[2*]

[1]Inonu University, Engineering Faculty, Computer Engineering Department, Malatya, Türkiye
[2]Inonu University, Engineering Faculty, Electrical and Electronics Engineering Department, Malatya, Türkiye

Keywords

Optimality, Robustness, Uncertain Systems, Control Design, Fractional Order Control, Bode's Ideal Loop.

Abstract

Bode's ideal loop models have been utilized in control system designs to obtain performance robustness for the Direct Current (DC) gain variations. However, effects of crossover frequency and fractional order on control optimality of Bode's ideal loop reference models have not been sufficiently discussed, and it may raise a question of whether a control system design based on Bode's ideal loop reference model is optimal. In this regard, this study revisits Bode's ideal loops to investigate Integral Square Error (ISE) optimality of Bode's ideal loops. For this purpose, the ISE optimality of Bode's ideal loop is theoretically investigated by using Parseval's theorem, and an ISE optimality condition is suggested in terms of crossover frequency and fractional order. Then, a generic controller family, which achieves an exact matching with the characteristics of the ISE optimal Bode's ideal loop, was implemented for inverse fractional-order control of a class of minimum phase fractional order plant models. The authors present a numerical experiment on an ISE optimal Bode's ideal loop inverse (OBILI) controller, and the ISE optimality and performance robustness of the designed control system were investigated for closed-loop control of a heat furnace system model via Monte Carlo simulations.

BODE İDEAL DÖNGÜLERİNE YENİDEN BAKIŞ: BODE İDEAL DÖNGÜLERİNİN İNTEGRAL KARESEL HATA OPTİMALLİĞİ VE BODE İDEAL DÖNGÜ TERS KONTROLÖR TASARIMI

Anahtar Kelimeler

Optimallik, Dayanıklılık, Belirsiz Sistemler, Kontrol Tasarımı, Kesirli Dereceli Kontrol, Bode'nin İdeal Döngüsü.

Öz

Bode ideal döngü modelleri, Doğru Akım (DA) kazanç değişimleri için performans dayanıklılığı elde etmek amacıyla kontrol sistemi tasarımlarında kullanılmıştır. Bununla birlikte, geçiş frekansı ve kesir derecenin Bode ideal döngü referans modellerinin kontrol optimalliği üzerindeki etkileri yeterince tartışılmamıştır ve bu, Bode ideal döngü referans modeline dayanan bir kontrol sistemi tasarımının optimal olup olmadığı sorusunu gündeme getirebilir. Bu bağlamda, bu çalışma, Bode ideal döngülerinin İntegral Karesel Hata (ISE) optimalliğini araştırmak için Bode ideal döngülerini yeniden ele almaktadır. Bu amaçla Bode ideal döngünün ISE optimalliği Parseval teoremi kullanılarak teorik olarak araştırılmış ve geçiş frekansı ve kesir derece açısından bir ISE optimallik koşulu önerilmiştir. Daha sonra, ISE optimal Bode ideal döngünün karakteristikleri ile tam bir eşleşme sağlayan bir genelleştirilmiş kontrolör ailesi, minimum faz kesir dereceli sistem modellerinin bir sınıfının ters kesir dereceli kontrolü için uygulanmıştır. Yazarlar, ISE optimal Bode ideal döngü ters (OBILI) kontrolörü üzerinde nümerik bir deney sunmuştur ve tasarlanan kontrol sisteminin ISE optimalliği ve performans dayanıklılığı, Monte Carlo simülasyonuyla bir ısı fırını sisteminin kapalı döngü kontrolü için araştırılmıştır.

Alıntı / Cite

Alagöz, B.B., Deniz, F.N., Keleş, C., (2025). Revisiting Bode's Ideal Loops: Integral Square Error Optimality of Bode's Ideal Loops and Bode's Ideal Loop Inverse Controller Design, Journal of Engineering Sciences and Design, 13(1), 202-220.

Yazar Kimliği / Author ID (ORCID Number)

B. B. Alagöz, 0000-0001-5238-6433
F. N. Deniz, 0000-0002-2524-7152
C. Keleş, 0000-0002-6818-7970

Makale Süreci / Article Process	
Başvuru Tarihi /Submission Date	13.03.2024
Revizyon Tarihi / Revision Date	12.10.2024
Kabul Tarihi / Accepted Date	08.01.2025
Yayım Tarihi / Published Date	20.03.2025

* Corresponding author: cemal.keles@inonu.edu.tr, +90-422-377-4797

REVISITING BODE'S IDEAL LOOPS: INTEGRAL SQUARE ERROR OPTIMALITY OF BODE'S IDEAL LOOPS AND BODE'S IDEAL LOOP INVERSE CONTROLLER DESIGN

Barış Baykant ALAGÖZ[1], Furkan Nur DENİZ[2], Cemal KELEŞ[2†],
[1]Inonu University, Engineering Faculty, Computer Engineering Department, Malatya, Türkiye
[2]Inonu University, Engineering Faculty, Electrical and Electronics Engineering Department, Malatya, Türkiye

Highlights

- This study revisits Bode's ideal loop and considers control performance limitations.
- Integral Square Error (ISE) optimality of Bode's Ideal Loop is discussed.
- An ISE optimal Bode's Ideal Loop inverse controller design scheme is illustrated.
- This generic controller allows optimal and robust closed loop system designs.

Purpose and Scope

The manuscript revisits the Bode's ideal loop reference model in aspects of ISE optimality and performance robustness and introduces an optimal Bode's ideal loop reference model based fractional order control system design for control robustness against parametric perturbation of the system model. It addresses elements of robust control according to the model based control design approaches. It introduces an easy-to-design ISE optimal Bode's ideal loop inverse (OBILI) controller for the control of a class of fractional order plant models.

Design/methodology/approach

Bode's ideal loops have been utilized in control system designs as a reference model in order to obtain a performance robustness for the gain variations of the control systems. However, control optimality of Bode's ideal loop reference models has not been sufficiently discussed in previous works. An investigation on whether Bode's ideal loop reference model is optimal in terms of the closed loop control error can be useful for controller design domain. This study firstly investigates the control optimality of Bode's ideal loops in terms of the Integral Square Error (ISE) and suggests a generic controller family that allows an exact matching of the control system characteristics with the characteristics of the ISE optimal Bode's ideal loop.

Findings

We firstly introduce an ISE optimal Bode's ideal loop inverse (OBILI) controller for the control of a class of fractional order plant models. The ISE optimality of the fractional order control system can inherently be achieved in the controller design task. This reference model based design approach significantly facilitates the optimal fractional order control system design with robustness assets of Bode's ideal loops.

Originality

We revisit the Bode's Ideal Loops and deeply discuss the robust control performance limitations of feedback control loops. Thus, we contributed to the brief discussion of Åström paper on the performance limitations of control loops in terms of control robustness and optimality. A design example of the proposed OBILI controller is illustrated for the optimal and robust closed loop control of a heat furnace system model. Rigorous robustness analysis is carried out by means of Monte Carlo simulations for parametric system uncertainties. Thus, the robust control performance improvements associated with the Bode's ideal loop based design is shown by using statistical performance assessments.

† Corresponding author: cemal.keles@inonu.edu.tr, +90-422-377-4797

1. Introduction

Robust control performance is essential for practical control system applications. Parametric variations, external disturbance, and measurement noise can deteriorate the real-world performance of the controllers that are designed theoretically optimal according to a nominal mathematical model of the controlled systems. Even if a control system is designed optimally, several factors (e.g., limitations of mathematical modeling, non-ideality in the realization of system elements, uncertainty in operation conditions, and system faults) can lead to deterioration of theoretically ensured control optimality in real-world control applications. To maintain practical control optimality in real-world control systems, a robust performance design paradigm plays an important role. Therefore, robust control has turned into a prominent topic of control engineering(Faisal et al., 2021; Zhou et al., 1998). The fractional order control works have aimed to resolve issues associated with the robustness of control system performance. Thus, the consideration of Bode's ideal loop in control(Åström, 2000; R. Barbosa et al., 2004; R. S. Barbosa et al., 2004; Bode, 1945; Bower & Schultheiss, 1961; Horowitz, 1963) and a closely related property of the phase response flatness, so-called iso-damping property(Y. Chen et al., 2005; Y. Q. Chen et al., 2006; J.-H. Cho & Hwang, 2007; Feliu-Batlle & Castillo-García, 2014) emerged as a central concern in optimal fractional order control system design problems(Li & Chen, 2008; Luo & Chen, 2009; Saha et al., 2010). The frequency domain loop shaping design methodologies have been utilized in the realization of the iso-damping property in fractional order control systems by providing flatness of phase response characteristics of open loop transfer function at the vicinity of the crossover frequency(Luo & Chen, 2009; Saha et al., 2010; Vinagre et al., 2003). To achieve the phase flatness objective, the following constraint has been popularly employed in optimal fractional order controller design problems(Luo & Chen, 2009):

$$\left(\frac{d\angle L(j\omega)}{d\omega}\right)_{\omega=\omega_c} \cong 0, \tag{1}$$

where the function $L(j\omega)$ stands for the frequency response of the open loop transfer function of a closed-loop fractional order proportional integral derivative (FOPID) control system. This classical negative feedback control loop involves a controller function $C(j\omega)$ and the controlled system function $G(j\omega)$, where the open loop transfer function is simply expressed in the form of $L(j\omega) = C(j\omega)G(j\omega)$. As in Eqn. 1, the phase response of the $L(j\omega)$ is denoted by $\angle L(j\omega)$. The crossover frequency ω_c is calculated according to the angular frequency ω that satisfies the condition of $|C(j\omega_c)G(j\omega_c)| = 1$.

Previously, the robust control performance limitations of feedback control loops were progressively discussed on the basis of a transfer function formalism of negative feedback control loops by Horowitz's book(Horowitz, 1963) and Åström in a tutorial paper (Åström, 2000). Åström stated that the properties of the open loop transfer function $L(j\omega)$ impose some limitations in terms of control robustness. Since the real processes mainly have control responses in the low frequency part of the frequency spectrum, their closed-loop control systems are designed to work in the low frequency region, and therefore all features linked with the control performance can be characterized according to the spectral properties within the low frequency region. Specifically, Åström emphasized that major properties associated with the control performance were characterized around the crossover frequencies of the control system (Åström, 2000). In the loop shaping design of control systems, the phase and gain crossover frequencies are mainly considered: The phase crossover frequency (ω_{pc}) of a system is the frequency at which the phase of the system first reaches $-\pi$ rad (−180°) and the gain crossover frequency (ω_c) is defined as the frequency where the amplitude of the open loop transfer function becomes a value of 1 (Bolton, 2004). As a major control property, the stability of the control system is guaranteed with positive phase and gain margins that can be calculated according to the phase and amplitude response characteristics of the open loop transfer function at the crossover frequencies (Bolton, 2004; Doyle et al., 1990; Wang et al., 2009).

Another useful control property related with the crossover frequency has emerged as the flatness of phase response characteristic of open loop transfer functions around the gain crossover frequency and this design property was considered as iso-damping property and utilized for system robustness in the loop shaping designs (Y. Chen et al., 2005; Feliu-Batlle & Castillo-García, 2014). However, its origin has traced back to Bode's works on feedback amplifiers, where it was discussed as the ideal cut-off characteristic to design robust amplifier circuits for DC gain variations (Åström, 2000; Bode, 1945; Doyle et al., 1990). In its historical progress, Bower and Schultheiss (Bower & Schultheiss, 1961), Horowitz (Horowitz, 1963), and (Alagoz et al., 2013) considered this property from a control point of view. Then, Åström presented a comprehensive investigation of Bode's ideal loop transfer function to discuss the robustness limitations of classical negative feedback control loops (Åström, 2000). Then, the terms of Bode's ideal loop transfer function have been phrased for control systems, and the phase response flatness of the open loop transfer function at crossover frequency has been investigated in more detail for control system design (Åström, 2000). Afterward, Bode's ideal loop was considered as a reference model in order to tune controller parameters to improve the time response of closed-loop control systems (Alagoz et al.,

2013; Doğruer et al., 2017; Saidi et al., 2015; Zhang et al., 2020). Recently, Bode's ideal loop transfer function has been preferred as a reference transfer function model to achieve phase flatness and performance robustness in loop shaping design (Fergani, 2022; Li et al., 2020; Sahoo & Mishra, 2021; Zheng et al., 2020; Zhuo-Yun et al., 2020).

This study aims to revisit discussions on the control performance robustness of Bode's ideal loop and extend these discussions to address the control optimality of Bode's ideal loop reference models. In this manner, parameters of the Bode's ideal loop are studied to figure out an optimal reference model. Thus, a control system design based on Bode's ideal loop reference model can inherently achieve the ISE optimality. For this purpose, ISE performance of the closed-loop control error is considered in the frequency domain as the total spectral energy of the control error by using Parseval's theorem, and then the total spectral energy of the control error is numerically minimized to determine the optimal crossover frequency and the fractional order parameters of the Bode's ideal loop reference models.

To demonstrate the benefits of the optimal Bode's ideal loop reference model for the optimal and robust controller design, we present an ISE optimal Bode's ideal loop inverse (OBILI) controller design example for the control of a class of minimum phase fractional order plant models. A numerical experiment is conducted to investigate optimal and robust control of a fractional order heat furnace system model. Monte Carlo simulations are conducted to show performance improvements of the ISE-OBILI controller in the on to performance of an optimal FOPID controller design.

2. Analyses on Bode's Ideal Loops

2.1. Preliminary Knowledge: Effects of Bodes Ideal Loop Parameters on System Stability and Robustness

The open loop transfer function of Bode's ideal loop is defined as

$$L(s) = \left(\frac{\omega_c}{s}\right)^{\alpha}, \tag{2}$$

where the parameter ω_c denotes crossover frequency and the parameter α stands for the fractional order of Bode's ideal loop (Åström, 2000; Bode, 1945). It is indeed a fractional order system model. The closed-loop transfer function of this system model is widely expressed in the form of

$$T(s) = \frac{L(s)}{1+L(s)} = \frac{\omega_c^{\alpha}}{s^{\alpha}+\omega_c^{\alpha}}. \tag{3}$$

Interest in Bode's ideal loops has grown in the field of fractional order control topic for the last two decades because Bode's ideal loop has been considered as a reference model for the robust performance control system design tasks. To understand the underlying reasons of why the fractional order control community has preferred Bode's ideal loop for a reference response of the robust control systems, one should consider the frequency response of Bode's ideal loops in Figure 1.

Figure 1 depicts the Bode diagram of Bode's ideal loop that is composed by drawing phase and magnitude responses of the open loop transfer function. The figure illustrates the effects of the parameters ω_c and α on the frequency responses in log-log scales. The magnitude response of Bode's ideal loop is written by

$$20\log_{10}|L(j\omega)| = 20\alpha \log_{10}\left(\frac{\omega_c}{\omega}\right) = -20\alpha \log_{10}(\omega) + 20\alpha \log_{10}(\omega_c). \tag{4}$$

The phase response of Bode's ideal loop is written by

$$\angle L(j\omega) = -\frac{\pi}{2}\alpha\,. \tag{5}$$

Some important remarks associated with phase and amplitude responses of Bode's ideal loops for system engineering can be summarized:

(i) The magnitude response is a linear curve in the log-log graph and the slope of the magnitude curve is -20α dB/dec in this graph. The slope of the magnitude curve is adjustable only by the fractional order α. (According to Figure 1, the slope of magnitude curve can be expressed geometrically as $-\frac{20\alpha \log_{10}(\omega_c)}{\log_{10}(\omega_c)} = -20\alpha$ dB/dec). This demonstrates the independence of the magnitude slope from the crossover frequency ω_c. Therefore, a change in the crossover frequency, which implies the change in the DC gain of Bode's ideal loop, does not affect the slope of

the magnitude curve and the associated properties. Besides, by considering Eqn. 5, it is evident that the phase response of Bode's ideal loop is also independent of the crossover frequency ω_c. These are the mathematical origins of the performance robustness of Bode's ideal loops for the crossover frequency variations. Therefore, with consideration of Eqn. 2, a change in the open loop gain of Bode's ideal loop is possible by altering only the crossover frequency ω_c, and this alteration does not affect the phase response and accordingly the phase margin that is $\varphi_m = -(\pi/2)\alpha + \pi$ (Bode, 1945). This effect validates the claims that have been suggesting that phase margin is independent of the open loop gain variation of Bode's ideal loop. Consequently, one concludes that the Bode's ideal loop is robust stable for any change in the crossover frequency.

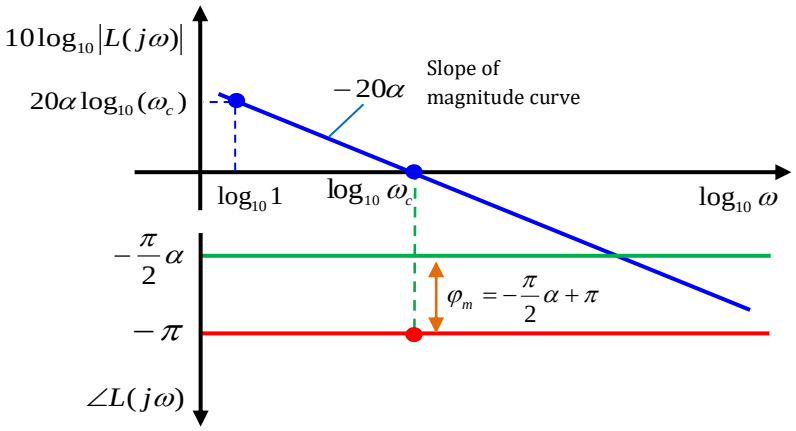

Figure 1. Bode diagram drawing of the Bode's ideal loop in logarithmic scales and illustrations of some important characteristic points related to control system performance

(ii) When the phase margin $\varphi_m = -(\pi/2)\alpha + \pi$ is considered, it is evident that Bode's ideal loop is always stable because of presenting a positive phase margin in the fractional order range of $0 \leq \alpha < 2$. Therefore, the range $0 \leq \alpha < 2$ guarantees the robust stability of Bode's ideal loops (Bode, 1945).

To validate these conclusions in frequency response plots, magnitude responses, phase responses and phase margins of Bode's ideal loops are drawn for $\omega_c = 10$, $1 \leq \omega \leq 100$ and different values of α in the range of [0,2] with 0.1 increments in Figure 2. The figure clearly shows that Bode's ideal loop is stable for $0 \leq \alpha < 2$ because of having a positive phase margin in this range.

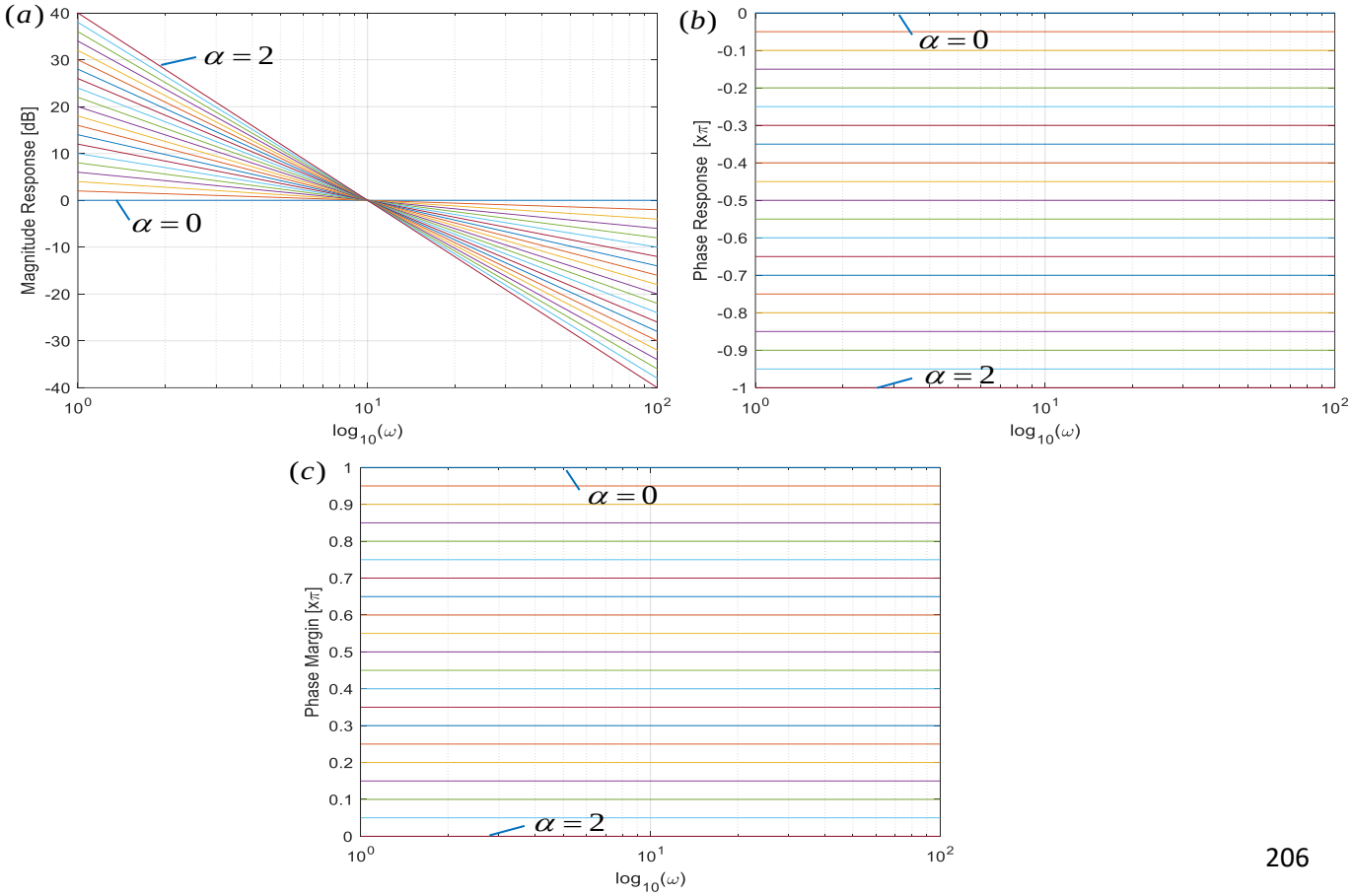

Figure 2. Magnitude responses (a), phase responses (b) and phase margins (c) of the Bode's ideal loops for various $\alpha \in [0,2]$ at $\omega_c = 10$

To show the effects of the crossover frequency ω_c, Figure 3 shows magnitude responses and phase responses of Bode's ideal loop for $\alpha = 1$ and various values of ω_c in the range [1,100] with 10 rad/sec increments. One can observe that there isn't any geometrical dependence between the phase response curve and the magnitude response curve in the case of the constant fractional order. For this reason, any change in ω_c, namely the DC gain of the open loop Bode's ideal loop, does not affect the phase response and the phase margin of the system according to Figure 3(b). This property may give a degree of freedom for tuning the parameter ω_c without concerning the stability of Bode's ideal loop in controller design efforts. In addition, this property confirms the insensitivity of the phase response to the gain variation.

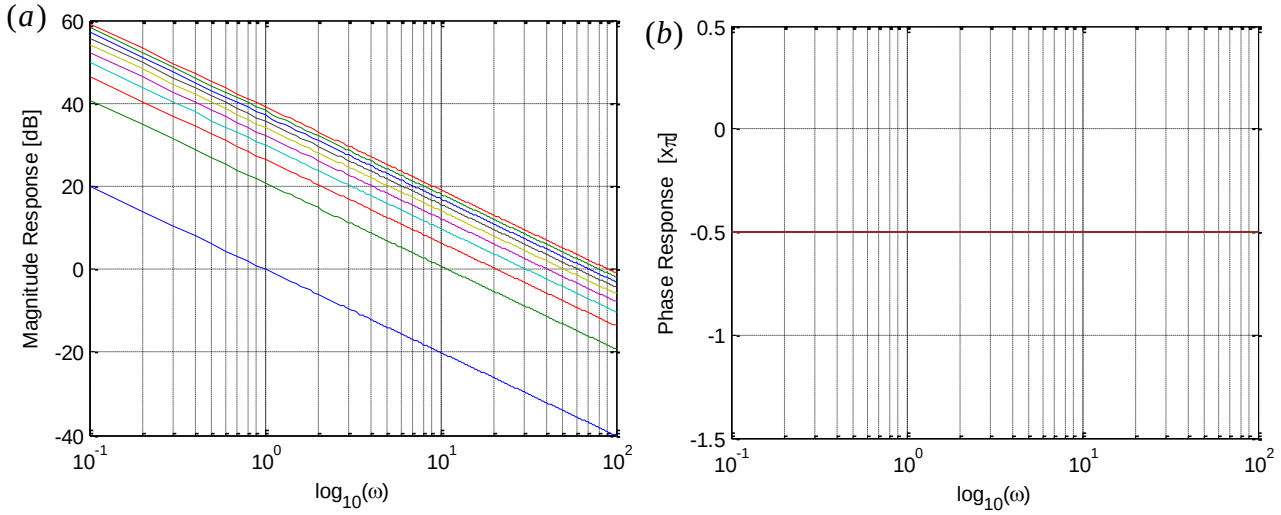

Figure 3. Magnitude responses (a) and phase responses (b) of Bode's ideal loops for $\alpha = 1$ and various values of ω_c in the range of [1,100] (These figures confirm that phase response is independent of ω_c)

2.2. Integral Squared Error Optimality of Bode's Ideal Loop

Bode's ideal loops have been used as a reference model in control system tuning problems (Alagoz et al., 2013; Doğruer et al., 2017; Yumuk et al., 2019; Zhang et al., 2020) because of expectations of their robust control assets that have been elaborated in the previous section. Although it has been utilized in many works, the control optimality of Bode's ideal loop reference models has not been adequately discussed. This section is particularly devoted to investigate the ISE performance optimality of Bode's ideal loops. In this aspect, we consider the ISE control performance of closed-loop Bode's ideal loop reference models and numerically solve the associated optimization problem in order to determine the optimal parameters of Bode's ideal loop, which minimize the integral of the square error. The aim of this effort is to figure out a Bode's ideal loop configuration (fractional order and crossover frequency values) that can simultaneously offer two features: (i) ISE optimality in time response, (ii) robustness for the gain variation (crossover frequency) of Bode's ideal loop reference model.

This effort can facilitate the solution of optimal controller design problems because ISE optimality will have been inherently provided by using the ISE optimal Bode's ideal loop reference model. Thus, there will be no need for solving an additional ISE optimality problem for the controller tuning when the time and frequency responses of the designed control system entirely resemble the response of the ISE optimal Bode's ideal loop reference model.

Let us express the error function of the closed-loop Bode's ideal loop by considering Eqn. 2 in the Laplace transform of $e(s) = R(s) - T(s)R(s)$, where the closed-loop transfer function is $T(s) = \frac{L(s)}{1+L(s)}$, one can write

$$e(s) = \frac{1}{1+L(s)}R(s) = \frac{1}{1+\left(\frac{\omega_c}{s}\right)^{\alpha}}R(s), \qquad (6)$$

where $R(s)$ represents the input of the closed-loop transfer function of the Bode's ideal loop. The ISE is commonly calculated by using the closed-loop control error signal $e(t)$ when a unit step input signal $r(t) = u(t)$ is applied to the input of the control loop. (Laplace transform of unit step input $r(t) = \mathrm{u(t)}$ is $\mathrm{R(s)} = \mathcal{L}\{\mathrm{u(t)}\} = 1/\mathrm{s}$) In the case of simulation or experimental data, the finite time ISE (Åström, 2000)was then used in the form of

$$E_T = \int_0^T e(t)^2 dt. \quad (7)$$

This formulation of the ISE is useful for performance analyses of the simulation or experimental data that was obtained for a finite observation period T. However, the selection of the observation period influences the results of finite time ISE calculations. An absolute ISE definition, which can be independent of the observation period, is written by

$$E_\infty = \int_{-\infty}^{+\infty} e(t)^2 dt. \quad (8)$$

By using the Parseval's theorem, E_∞ can be expressed in the frequency domain as (Kealy & O'dwyer, 2003; Merrikh-Bayat, 2012)

$$E_\infty = \int_{-\infty}^{+\infty} e(t)^2 dt = \frac{1}{2\pi}\int_{-\infty}^{+\infty} |e(j\omega)|^2 d\omega, \quad (9)$$

where $e(j\omega) = e(s)|_{s=j\omega}$ are used in Eqn. 9, then the absolute ISE of Bode's ideal loop can be written as

$$E_\infty = \frac{1}{2\pi}\int_{-\infty}^{+\infty} \left| \frac{1}{1+\left(\frac{\omega_c}{j\omega}\right)^\alpha} \frac{1}{j\omega} \right|^2 d\omega. \quad (10)$$

Finally, the ISE optimal Bode's ideal loop parameter can be found by solving the following optimization problem:

$$\min E_\infty(\omega_c, \alpha) = \frac{1}{2\pi}\int_{-\infty}^{+\infty} \left| \frac{1}{1+\left(\frac{\omega_c}{j\omega}\right)^\alpha} \frac{1}{j\omega} \right|^2 d\omega \quad (11)$$

We solved this optimization problem by using Brute force search. The Brute force search method searches all evenly sampled solutions from a low dimensional search space. The Brute force search is a useful and proven search technique when there is a need for ~~a~~ discrete performance mapping within the search space. Thus, one can explore all optimal points within the sampled finite search spaces, and previously, it was effectively used in the fractional order control system stabilization tasks (Alagoz, 2018; Matušů et al., 2018). In the current application, for sampled values of ω_c and α parameters in a finite search range, the absolute ISE of Bode's ideal loop was numerically calculated by using the numerical integral function of the Matlab program. For the consistent numerical calculation of Eqn. 11, the numerical integral was performed for a sufficiently large range of the angular frequency ($[-10^{10}, 10^{10}]$) compared to the sampling ranges of ω_c and α parameters. Thus, the accuracy of the numerical integration in Eqn. 11 can be maintained. (The Matlab code for the numerical calculation of Eqn. 11 is also provided in the Appendix section.)

Figure 4 shows the distribution of $E_\infty(\omega_c, \alpha)$ in the ranges $\omega_c \in [1,10000]$ with 10 rad/sec increments and $\alpha \in [0,2]$ with 0.1 increments. The figure depicts an ISE performance mapping of closed-loop Bode's ideal loops. In the figure, the minimum ISE was obtained 5.10^{-4} and the optimal model parameters were found $\omega_c^* = 1000$ and $\alpha^* = 1$. The same computations were carried out by increasing the range of ω_c and results are listed in Table 1. Results reveal that the optimal value of the fractional order is $\alpha^* = 1$ and optimal values of crossover frequency go consistently to the highest ω_c frequencies that are the upper boundary of the search range of ω_c. According to these numerical results, one can easily infer that the optimal value of the crossover frequency goes to the infinite frequency, $\omega_c^* \to \infty$, in the case that the Brute search range of ω_c expands to infinity. Consequently, the conditions $\alpha^* = 1$ and $\omega_c^* \to \infty$ are sufficient to ISE optimality of Bode's ideal loops. By considering these findings, the open loop transfer function of the ISE optimal Bode's ideal loop can expressed by using the condition $\alpha^* = 1$ and $\omega_c^* \to \infty$ as

$$L^*(s) = \left(\frac{\omega_c}{s}\right)|_{\omega_c^* \to \infty}. \quad (12)$$

Then, a transfer function of the optimal ISE Bode's ideal loop can be written by

$$T^*(s) = \frac{\omega_c^*}{s+\omega_c^*} = \frac{1}{\frac{1}{\omega_c^*}s+1}|_{\omega_c^* \to \infty}. \quad (13)$$

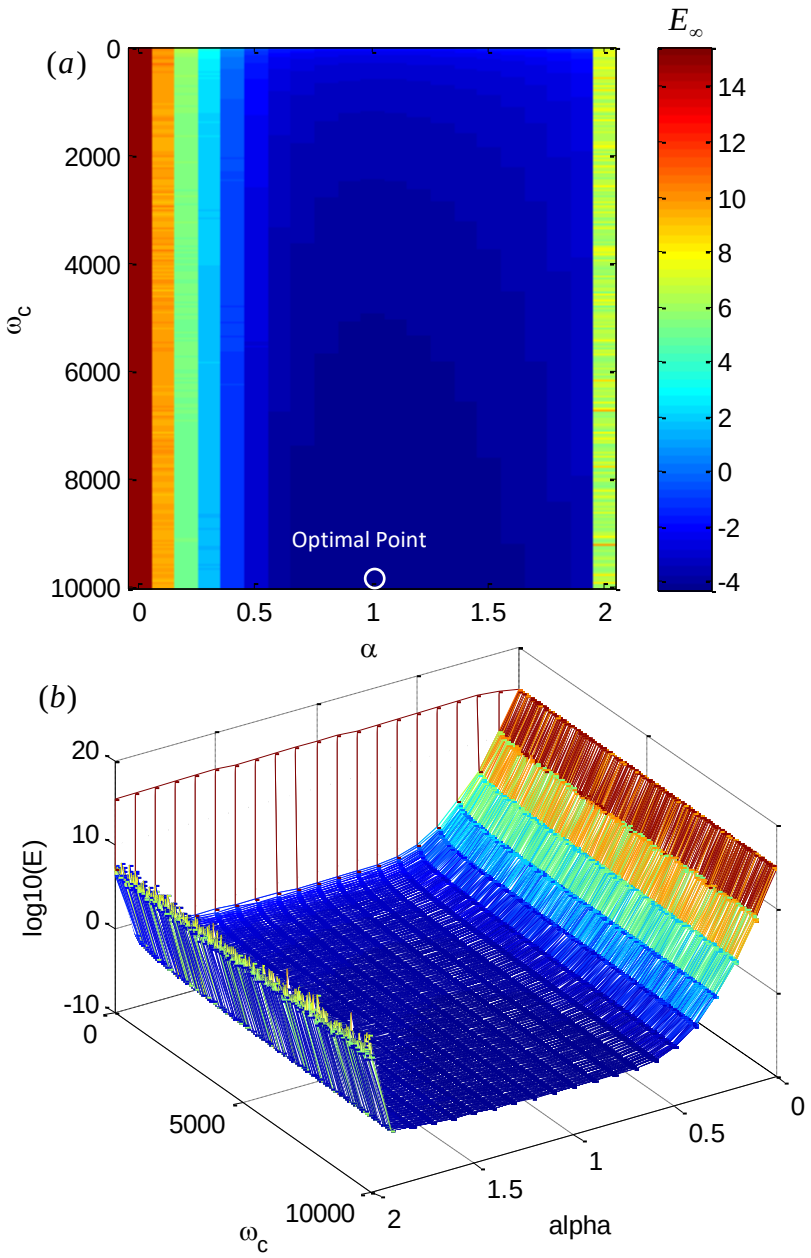

Figure 4. Logarithmic scale distribution $E_{\infty}(\omega_c, \alpha)$ in the ranges $\omega_c \in [1, 10000]$ with 10 rad/sec increment and $\alpha \in [0, 2]$ with 0.1 increments ((a) top view and (b) side view)

According to Eqn. 13, the optimal ISE Bode's ideal loop is theoretically an infinite bandwidth, first order transfer function because of the requirement of $\omega_c^* \to \infty$. This indeed implies a unit transfer function, $T^*(s) = 1$, namely an ideal closed-loop transfer function. The unit transfer function represents an ideal lossless system with an infinite bandwidth and a zero-time constant. However, the unit transfer function is a conceptual model because the infinite crossover frequency is not possible in real-world or practical control systems. From a practical point of view, ISE performances of real systems are bounded with a finite crossover frequency specification. To improve ISE performances of real control system design methodologies, which are using optimal ISE Bode's ideal loop functions ($T^*(s)$ or $L^*(s)$) as a reference model, one should consider maximization of the ω_c. As a consequence, an essential limitation for the optimality of Bode's ideal loop comes from the finite ω_c specifications of the real-world control systems. This is a result that also confirms the view of Åström, which has been suggested the crossover frequency to be an essential limitation for real-world control performance (Åström, 2000).

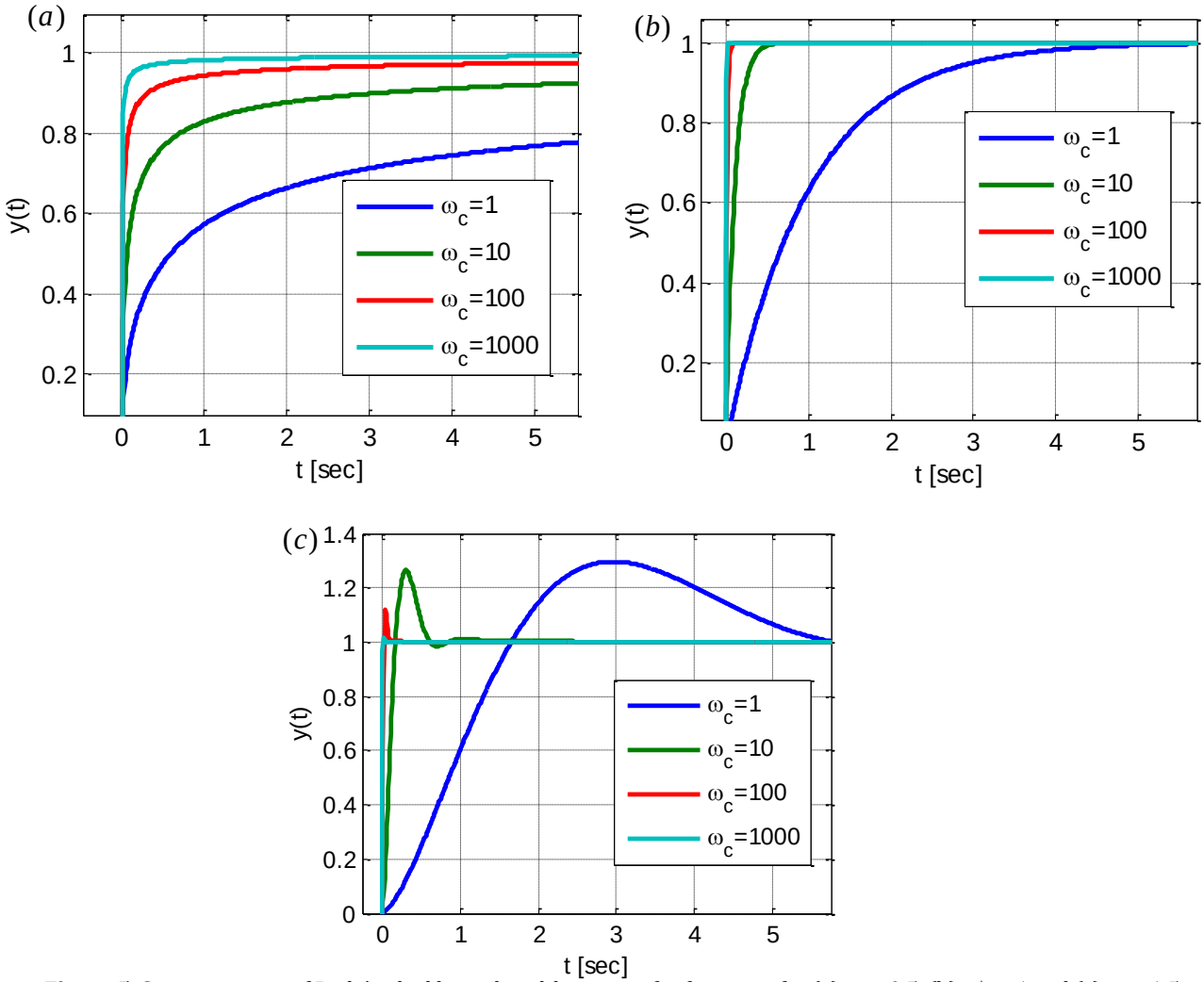

Figure 5. Step responses of Bode's ideal loop closed-loop transfer functions for (a) $\alpha = 0.5$, (b) $\alpha^* = 1$ and (c) $\alpha = 1.5$

Figure 5 shows step responses of the closed-loop transfer functions of Bode's ideal loop for various crossover frequencies and different fractional orders. (FOTF toolbox was used to perform the step response simulations (Xue, 2017). These step responses in the figure validate the results in Table 1. The ISE performance of Bode's ideal loop is the best at $\alpha^* = 1$ because the control error $|e(t)| = |1 - y(t)|$ is the lowest for $\alpha^* = 1$ for the same values of the ω_c. In the figure, an increase in the crossover frequency can improve the ISE performance in general. However, the crossover frequency of real-world systems is finite and limited. When this limitation of real-world control systems is taken into account, Bode's ideal loop with $\alpha^* = 1$ promises the best ISE control performance at a given crossover frequency of the system. It is a noteworthy point that Bode's ideal loops offer robust stability in the case of crossover frequency variations as shown in the figure.

Table 1. Minimum ISE search results for the various range of ω_c

Search range of ω_c	ω_c^*	α^*	Minimum ISE
$\omega_c \in$[1,10]	10	1	510^{-2}
$\omega_c \in$[1,100]	100	1	5.10^{-3}
$\omega_c \in$[1,1000]	1000	1	5.10^{-4}
$\omega_c \in$[1,2000]	2000	1	$2.5.10^{-4}$
$\omega_c \in$[1,5000]	5000	1	$9.99.10^{-5}$
$\omega_c \in$[1,10000]	10000	1	$4.99.10^{-5}$

3. Numerical Experiments

3.1. An ISE Optimal Bode's Ideal Loop Inverse Controller Design for Minimum Phase Plant Models

This section presents an inverse controller design example, which is based on the ISE Optimal Bode's ideal loop reference model. To observe the contributions of Bode's ideal loop reference model, the open loop transfer function of the control system exactly matches the open loop transfer function of ISE optimal Bode's ideal loop and this assures fully matching of frequency responses. Accordingly, this controller structure is referred to as ISE Optimal Bode's Ideal Loop Inverse (OBILI) controller in this study. The inverse control is based on the utilization of an inverse model of the plant function for the controller design. (It was also known as the direct synthesis method (Fergani, 2022). Previously, the inverse control strategy has been applied in the control systems (J. Cho et al., 2006; Deniz, 2022; Fergani, 2022; Nagarsheth & Sharma, 2020; Saxena & Biradar, 2022; Shafiq, 2005; Yadav & Hirenkumar, 2022; Yumuk et al., 2016; Zheng et al., 2020) and it has been implemented in conjunction with several control system types such as in fuzzy control systems (Kumbasar et al., 2011), in neural network control (Narendra & Parthasarathy, 1990), in PID controller design (Chakraborty et al., 2020; Jeng & Lin, 2012). A Smith predictor based fractional-order PI control law is suggested by using direct synthesis (Vu & Lee, 2014). The second generation CRONE controller design has also been utilized from the inverse controller design scheme (Lanusse et al., 2013). In this section, we illustrate a generic inverse controller structure that exactly matches with the frequency response of ISE optimal Bode's ideal loop for minimum phase plant models.

For this purpose, the open loop transfer function is matched with Bode's ideal loop transfer function as follows:

$$C(s)G(s) = \left(\frac{\omega_c}{s}\right)^{\alpha}. \tag{14}$$

Then, the Bode's ideal loop inverse controller is obtained as

$$C(s) = \frac{1}{G(s)}\left(\frac{\omega_c}{s}\right)^{\alpha}, \tag{15}$$

where the $C(s)$ is the inverse controller function and $G(s)$ is the plant function that is controlled by the controller $C(s)$ in a negative feedback loop (Zheng et al., 2020). Figure 6 shows a block diagram of the closed-loop control system with the inverse controller $C(s)$.

We assumed that the minimum phase plant function model is accurate and well-represent the real system response. Under this modeling assumption, it is investigated whether the loop shaping designs based on the ISE optimal Bode's ideal loop reference model can improve the robustness and optimality of the designed closed-loop control system. By matching with the optimal ISE Bode's ideal loop reference model, the designed control system inherits the frequency domain properties of Bode's ideal loop reference model; for instance, providing flattened phase response and a decrease of the magnitude response with almost a constant slope in log-log scales.

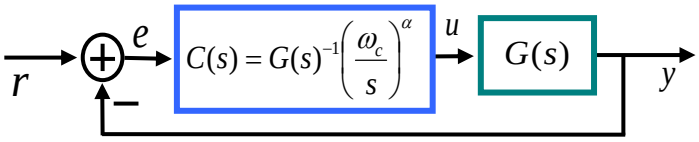

Figure 6. Block diagram of the closed-loop Bode's ideal loop inverse control

The findings of analyses in the previous section have demonstrated that the ISE optimality of Bode's ideal loop reference model is possible for $\alpha^* = 1$ and $\omega_c^* \to \infty$, the ISE OBILI controller can be expressed in the form of cascaded two functions as follows:

$$C(s) = G(s)^{-1}\left(\frac{\omega_c}{s}\right)_{\omega_c^* \to \infty}, \tag{16}$$

where $G(s)^{-1}$ is the inverse function of the plant model and the term $(\omega_c/s)_{\omega_c^* \to \infty}$ stands for the ISE optimal Bode's ideal loop reference model. (This term indeed performs an ideal integral operation with the infinite bandwidth.) Eqn. 16 reveals a design concern to improve the ISE optimality of this control system, that is, the maximization of crossover frequency ω_c.This maximization improves the ISE optimality without causing overshoots in settling. Thus, the OBILI controller function with Eqn. 16 achieves a control performance that allows an enhanced ISE optimality with an overshoot-free settling and the control robustness that allows insensitivity to the crossover frequency fluctuations of the control system.

In the literature, several approaches were proposed for the inverse control of non-minimum phase plant models. Minimum phase and non-minimum phase parts are separated (Arya & Chakrabarty, 2018) and approximated (Saxena & Biradar, 2022; Yadav & Hirenkumar, 2022; Yumuk et al., 2016). Works on Internal Model Control techniques have suggested effective solutions for dealing with non-minimum phase plant models (Arya & Chakrabarty, 2018; Kumbasar et al., 2011; Saxena & Hote, 2022). To illustrate a simplified design example for robust control performance analysis, we consider a class of minimum phase fractional order plant model that has been expressed in the form of

$$G(s) = \frac{1}{a_2 s^{\beta_2} + a_1 s^{\beta_1} + a_0}, \tag{17}$$

An analytical optimal FOPID controller design method has been proposed by Zhao et al. for this class of the fractional order plant model (Zhao et al., 2005). One can generalize this class of minimum phase plant function for n number of fractional elements as

$$G(s) = \frac{K}{a_n s^{\beta n} + a_{n-1} s^{\beta n-1} + \cdots + a_2 s^{\beta_2} + a_1 s^{\beta_1} + a_0}, \tag{18}$$

An ISE OBILI controller for this class of fractional plant function can be designed in a generic form by considering Eqn. 16 as,

$$C(s) = \left(k_n s^{\beta_n - 1} + k_{n-1} s^{\beta_{n-1} - 1} + .. + k_2 s^{\beta_2 - 1} + k_1 s^{\beta_1 - 1} + k_0 s^{-1}\right)_{\omega_c^* \to \infty}, \tag{19}$$

Then, one can rearrange this controller function to express it in a more elegant form as follows:

$$C(s) = \left(\frac{k_0}{s} + \sum_{i=1}^{n} k_i s^{\beta_i - 1}\right)_{\omega_c^* \to \infty}, \tag{20}$$

where the controller coefficients are $k_i = \frac{\omega_c a_i}{K}$. In fact, Eqn. 20 infers a generic fractional order controller that involves transformative fractional order elements: The term $s^{\beta_i - 1}$ infers a fractional order derivative element for$\beta_i > 1$, it transforms to a fractional order integral element in the case of $\beta_i < 1$and it becomes a constant gain element for $\beta_i = 0$. This flexibility of the generic OBILI controller structure allows for taking over all features of Bode's ideal loop reference model. Previously, generic model control has been studied and the advantage of generic model controller designs has been illustrated by Lee et al. (Kharrazi et al., 2012; Lee & Sullivan, 1988).

3.2. A Numerical Study for Control of a Heating Furnace System Model

In this section, we illustrate a design example for a fractional order nominal model of a heating furnace that was written by

$$G(s) = \frac{1}{14994 s^{1.31} + 6009.5 s^{0.97} + 1.93}, \tag{21}$$

where the nominal model parameters of the heating furnace according to Eqn. 18 are $K = 1$, $a_2 = 14994$, $a_1 = 6009.5$, $a_0 = 1.93$, $\beta_2 = 1.31$, $\beta_1 = 0.97$(Podlubny, 1994; Zhao et al., 2005). Let us design an OBILI controller with $\omega_c = 0.2$ rad/s for the plant function that is given by Eqn. 21. ($\omega_c = 0.2$ rad/s is suitable for physically implementable heating furnace control.) By considering Eqn. 20 and taking $n = 2$ for the number of fractional order elements in the plant function (Eqn. 21), the generic controller function can be written by

$$C(s) = \frac{k_0}{s} + k_1 s^{\beta_1 - 1} + k_2 s^{\beta_2 - 1}, \tag{22}$$

where controller coefficients are $k_2 = \omega_c a_2 / K = 0.2 \times 14994/1 = 2998.8$, $k_1 = \omega_c a_1 / K = 0.2 \times 6009.5/1 = 1201.9$ and $k_0 = \omega_c a_0 / K = 0.2 \times 1.93/1 = 0.3860$. Then, by using $\beta_2 = 1.31$ and $\beta_1 = 0.97$, the proposed OBILI controller becomes

$$C_{OBILI}(s) = 0.3860 s^{-1} + 1201.9 s^{-0.03} + 2998.8 s^{0.31}. \tag{23}$$

For the plant function (Eqn. 21), a FOPID controller has been designed in (Zhao et al., 2005) as follows:

$$C_{\mathrm{Z}}(s) = 736.8054 - 0.5885 s^{-0.6} - 818.4204 s^{0.35}, \tag{24}$$

Figure 7 shows Bode plots of the proposed OBILI control system and the optimal FOPID control system that was designed for a phase margin of $\frac{\pi}{3}$ rad and a gain margin of 1.1 by (Zhao et al., 2005). Zhao et al's approcah does not consider ISE optimality. One can see that the frequency responses of the Bode's ideal loop and the proposed OBILI control system completely match and therefore the OBILI control system takes all inherent properties of the optimal Bode's ideal loop such as the iso-damping property, independence of phase response from the crossover frequency of the system and ISE optimality for $\alpha^* = 1$. Specifically, the OBILI control system achieves complete phase flatness at $\frac{\pi}{2}$ rad in the phase response. However, Zhao et al.'s optimal FOPID control system provides a slight slope around the crossover frequency. These results show that the OBILI control system can provide control performance assets that are inherited from the ISE optimal Bode's ideal loop. Zhao et al.

Figure 8 shows unit step responses of the proposed OBILI controller and Zhao et al.'s FOPID controller from the control simulation of the heating furnace model. The OBILI control provides a faster settling without any overshoots and its step response can completely overlap with the step response of the closed-loop transfer function of the Bode's ideal loop. This result also confirms the matching of time response properties of the OBILI control system and Bode's ideal loop and inherits optimality and robustness assets of Bode's ideal loop in the time domain. The optimal FOPID control settles in a longer period by producing a slight overshoot. The figure clearly shows that the ISE optimality of the proposed OBILI control can also be preferable when compared to the ISE optimality of the Zhao et al.'s optimal FOPID control.

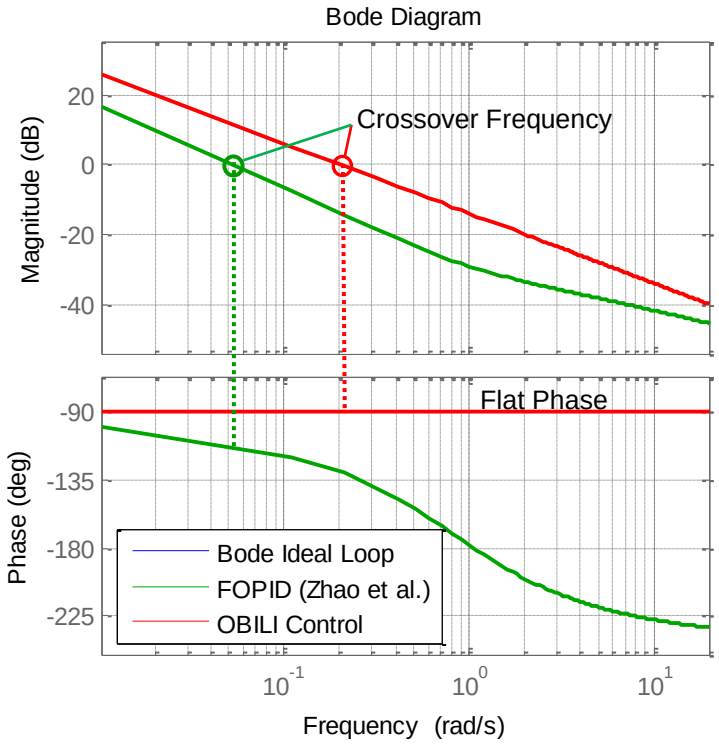

Figure 7. Frequency responses of the proposed OBILI control and the optimal FOPID control for the heating furnace model

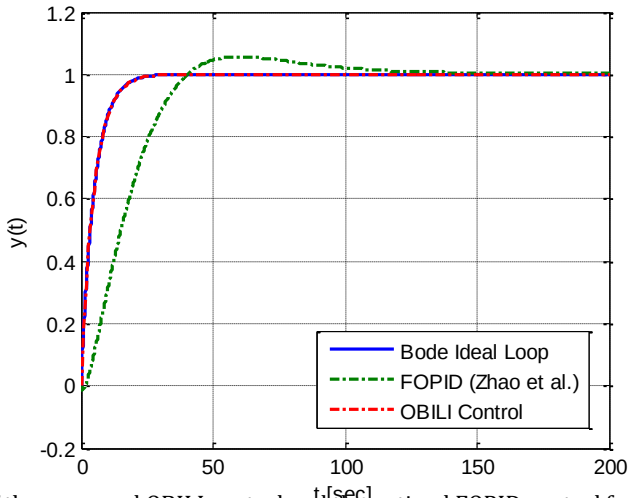

Figure 8. Unit step responses of the proposed OBILI control and the optimal FOPID control for the heating furnace model

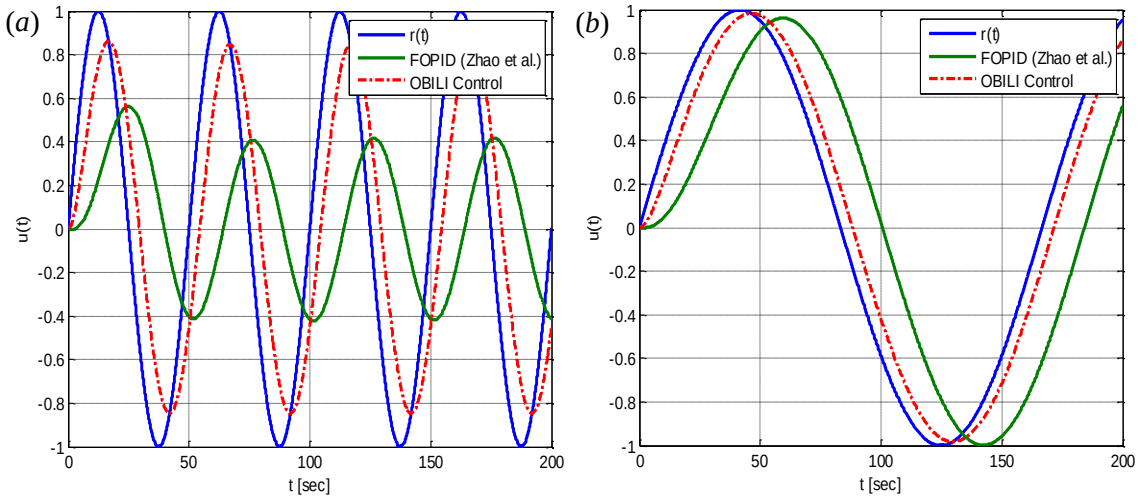

Figure 9. Time responses of the proposed OBILI control and the optimal FOPID control for sinusoidal reference inputs

To observe response of complete phase flatness at $\frac{\pi}{2}$ rad, sinusoidal reference signals with angular frequencies of 0.1257 rad/sec and 0.0377 rad/sec were applied, and responses of both controllers are illustrated in Figure 9. Since the crossover frequency of Zhao et al.'s FOPID control system is lower than the reference signal frequency 0.1257 rad/sec, it cannot well-track the reference signal amplitude, and the output amplitude is attenuated. (For attenuation-free control, the phase crossover frequency should be greater than the maximum operation frequency ω_{max} , accordingly the crossover frequency depending on application requirements can be selected according to application requirements as $\omega_c > \omega_{max}$) Since the phase response of the FOPID control system is not flat, varying phase delay is observed at the output of the FOPID control system for changing frequency of the reference input signal. However, the phase delay of the proposed OBILI control system is lower at these frequencies and it is almost constant when frequency of the reference signal is changed. This effect is called as the phase delay robustness that is related to the complete phase flatness property of OBILI control. It can also better track the sinusoidal reference signal because the crossover frequency of controller is greater than frequencies of sinusoidal waveforms in figures.

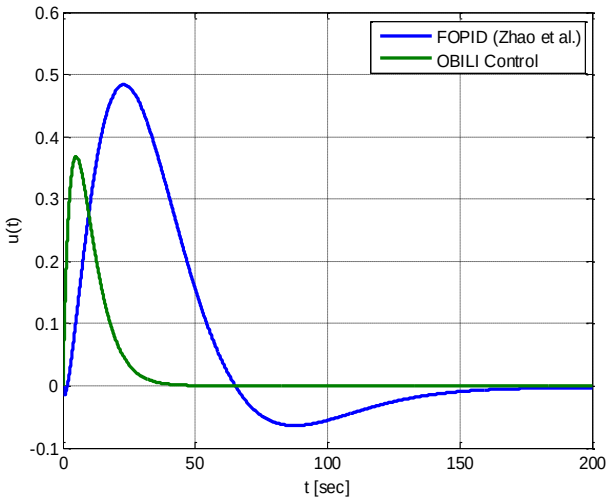

Figure 10. Control signals for the proposed OBILI control and the optimal FOPID control for the heating furnace model

Figure 10 shows control signals $(u(t))$ for the proposed OBILI and Zhao et al.'s FOPID controllers. The OBILI controller can achieve optimal control with lower amplitude and lower energy control signal compared to Zhao et al.'s FOPID controller.

It is useful to investigate the robust control performance of the control systems under the parametric perturbations of the plant model. Figure 11 shows the unit step responses of the proposed OBILI controller and the optimal FOPID controller (Zhao et al., 2005) for the parametric perturbation of the model coefficients. The gain coefficients $K = 1$ and $a_2 = 14994$ are increased 1.5 and 2 times to perform a high variability in these coefficients.

Then, we observed the sensitivity of the step responses to each variation in these coefficients to evaluate the control performance robustness of the control systems. The figure illustrates that the OBILI control can present a more robust step response performance than the optimal FOPID control for such variations in the gain coefficients. (Deviations in step responses of the OBILI control are less than those of optimal PID control) As discussed in the previous sections, this robust performance improvement is achievable because of inheriting all assets of Bode Ideal loops.

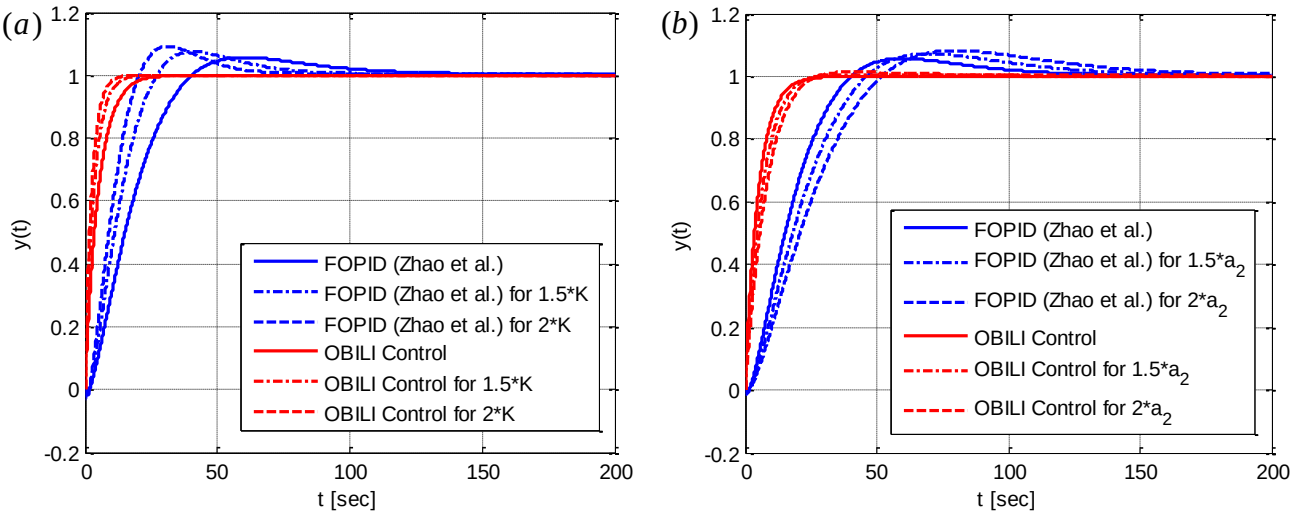

Figure 11. Changes in the unit step responses of the proposed OBILI control and the optimal FOPID control under parametric perturbations of the heating furnace model for the gain parameters K in (a) and the denominator coefficient a_2 in (b)

It is also valuable to consider changeability in step responses of the proposed OBILI controller and the optimal FOPID controller (Zhao et al., 2005) under the fractional model order perturbations. Figure 12 shows step responses of the proposed OBILI controller and the FOPID controller under parametric perturbations of the model orders β_1 and β_2. The order $\beta_1 = 0.97$ was changed to $1.2 \times \beta_1$ and $0.8 \times \beta_1$. The order $\beta_2 = 1.31$ is changed to $1.2 \times \beta_2$ and $0.8 \times \beta_2$ .These order variations can be assumed as a significant variation in the fractional order system dynamics. The step response of the OBILI controller is less affected by these order variations compared to the optimal PID controller. (Deviations in step responses of OBILI control is less than those of the optimal PID control) These numerical experiments indicate that the step response performance robustness of the OBILI control under the variations of the fractional model orders could be relatively better than those of the optimal FOPID control. Reasons for this improvement in robust control performance can be closely related to Bode's ideal loop properties that are associated with the phase response flatness (iso-damping property) and the constant slope of the magnitude curve. Another factor can be the higher crossover frequency of the OBILI control system.

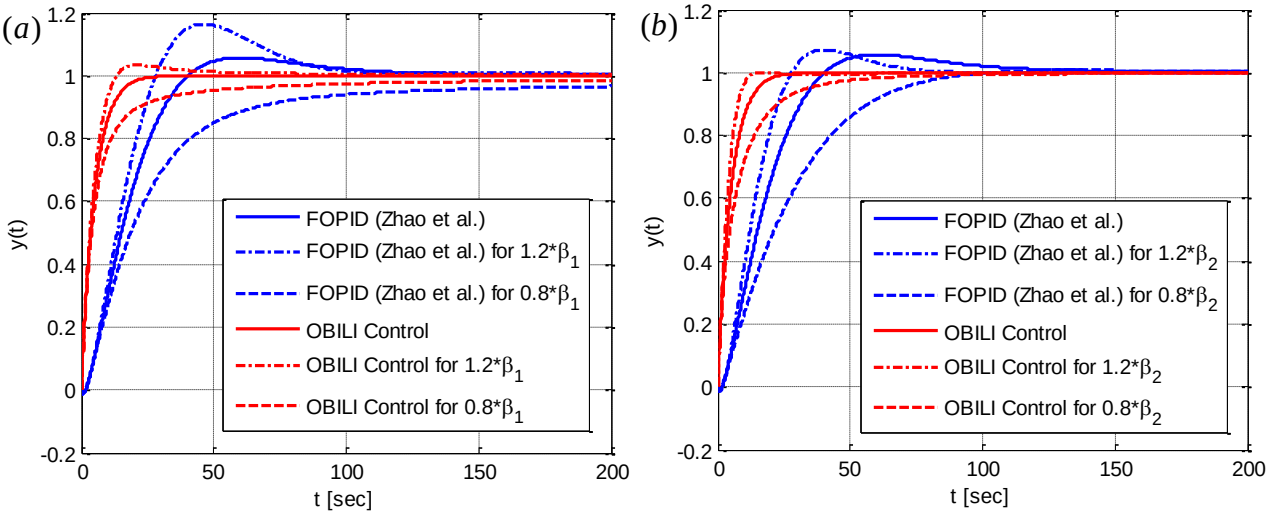

Figure 12. Changes in the unit step responses of the proposed OBILI control and the optimal FOPID control for parametric perturbations of the heating furnace model for the fractional order parameters β_1 in (a) and β_2 in (b)

Table 2 lists the ISE performances of the control systems under the parametric model perturbations that were illustrated in Figures 11 and 12. The ISE data in the table confirms both enhanced ISE optimality and the improved performance robustness of the proposed OBILI control system.

Table 2. ISE performances of the proposed OBILI control system and the optimal FOPID control system (Zhao et al., 2005) under some parametric model perturbations

Plant Model and Parametric Perturbations	The optimal FOPID Control System	The proposed OBILI Control System
ISE for the nominal system	113.25	25.75
ISE under $1.5 \times a_2$ coefficient perturbation	135.28	32.94
ISE under $2.0 \times a_2$ coefficient perturbation	155.86	39.85
ISE under $1.5 \times K$ coefficient perturbation	85.10	17.42
ISE under $2.0 \times K$ coefficient perturbation	70.41	13.25
ISE under $1.2 \times \beta_2$ fractional order perturbation	93.28	21.32
ISE under $0.8 \times \beta_2$ fractional order perturbation	157.31	36.26
ISE under $1.2 \times \beta_1$ fractional order perturbation	107.48	23.73
ISE under $0.8 \times \beta_1$ fractional order perturbation	147.39	32.76

3.3. Monte Carlo Simulations for Analysis of Control Performance Robustness

In order to more realistically analyze performance robustness in case of parametric perturbations of the fractional order heating furnace model, we randomly varied all parameters of the heating furnace model in the interval uncertainty ranges that involve±50% deviation range from nominal values of the gain coefficients and ±20% deviation range from nominal values of the fractional orders of the model. For these uncertainty ranges, the interval uncertain model of the heating furnace model can be expressed as.

$$G(s) = \frac{1}{[7497,22491\,]s^{[0.655,1.965]} + [3004.8,9014,3]s^{[0.485,1.455]} + [0.965,2.895]}. \qquad (25)$$

Accordingly, by performing 100 times uniform random sampling of the model parameters within the deviation ranges, 100 versions of parametric perturbed heating furnace model were randomly generated from the interval uncertain system model (Eqn. 25). Thus, a Monte Carlo simulation of the control robustness was carried out to observe the robustness of the step response and ISE performances. Figure 13 shows randomly sampled parameter distributions for each parameter of the heating furnace model.

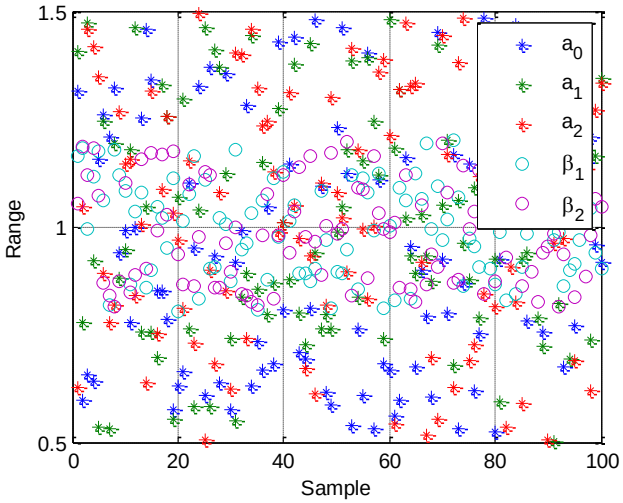

Figure 13. The random sampled parameter distributions from the interval uncertainty range to mimic unpredictable parametric perturbations of the heating furnace model

Figure 14 shows the unit step responses of the proposed OBILI controller and the optimal FOPID controller (Kharrazi et al., 2012) for all perturbed models. The dispersion in the step responses is less for the OBILI control than the dispersion in the FOPID control, and these results suggest that the OBILI control can respond more robustly to the parametric perturbation of the system model. The ISE performance distributions in Figure 15 confirm these results. Table 3 lists ISE performance statistics of the control systems for 100 randomly perturbed plant models and verifies the contributions of the proposed OBILI control to the improvement of robust control performance. Figure 16 shows the convergence of the average ISE of both control systems during the Monte Carlo simulation.

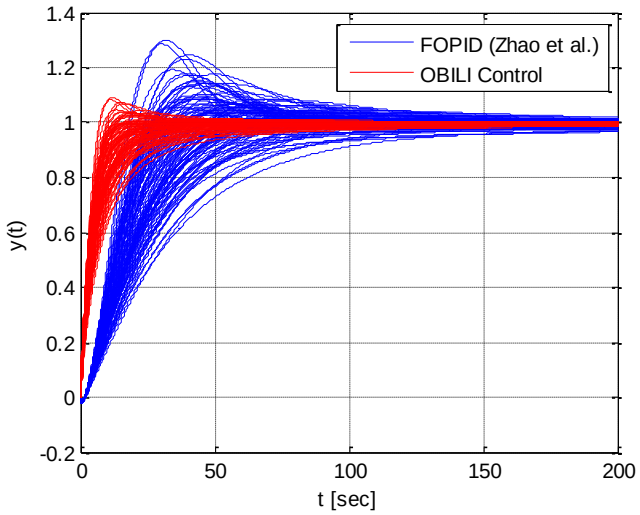

Figure 14. Unit step responses of the proposed OBILI controller and the optimal FOPID controller for all randomly perturbed versions of the heating furnace model

Table 3. Comparisons of ISE performance statistics for the proposed OBILI control system and Zhao et al.'s optimal FOPID control system

ISE Statistics	FOPID Control System	The proposed OBILI Control System
Mean value of ISE	124.07	28.29
Standard deviation of ISE	27.02	7.20
Maximum value of ISE	208.56	50.07
Minimum value of ISE	85.03	17.31

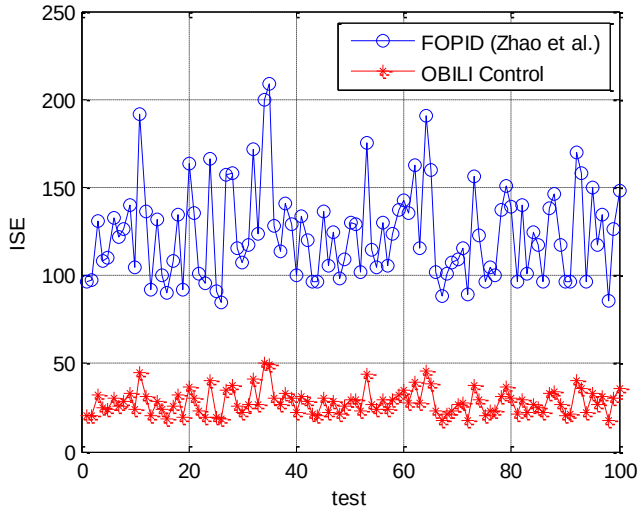

Figure 15. ISE performances of both control systems for 100 randomly perturbed versions of the heating furnace model

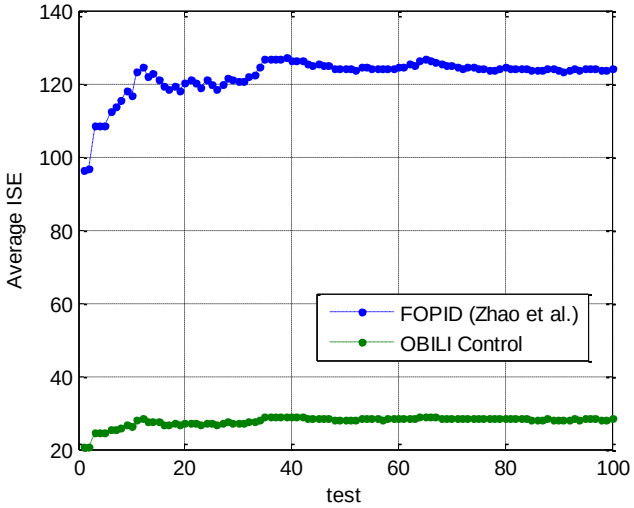

Figure 16. Convergence of average ISE performances of both control systems for all randomly perturbed versions of the heating furnace model from Monte Carlo simulation

4. Discussions and Conclusions

The fractional order control topic has come up with a robust control performance paradigm (Manabe, 1960). Loop shaping design methodologies based on Bode's ideal loop contribute to this paradigm. Although it has been used as a reference model in controller design to improve performance robustness, a detailed investigation of Bode's ideal loop itself is quite limited. In this fashion, we aim to revisit Bode's ideal loops in this study. After briefly surveying the role of Bode's ideal loops in the system design, the control optimality of Bode's ideal loop reference models was discussed. The author revealed a sufficient control optimality condition for closed-loop Bode's ideal loops by numerically solving the stated ISE optimization problem. The numerical solution of this optimization problem indicated that the fractional order value of 1 ($\alpha^* = 1$) and the highest possible value of the crossover frequency parameter (ideally $\omega_c^* \to \infty$) can enhance the ISE optimality of Bode's ideal loops. These findings are significant for controller design because of suggesting improvement in both performance robustness and the ISE optimality in the loop shaping controller design.

This study elaborated two assets of Bode's ideal loops for control system design practice: (i) performance robustness for gain variations and (ii) the ISE optimality. On the other hand, analysis results indicate an important performance limitation of control systems, that is, in order to improve the ISE control performance, maximization of the crossover frequency is required in Bode's ideal loop-based control system designs. This result confirms Åström's conjecture that suggests the crossover frequency of real systems as a limitation for control performance (Åström, 2000). The current study demonstrated the underlying mechanism of this limitation in relation with the optimality of Bode's ideal loops. We also conclude that an ideally optimal design with zero ISE requires an infinite bandwidth system due to the condition of $\omega_c^* \to \infty$. In reality; the finite crossover frequency nature of real-world systems introduces a physical limitation for the ISE optimality of the Bode's ideal loop-based control system designs.

Realization of fractional order elements is possible by using approximate equivalent models today. OBILI controller models for the non-minimum phase plant are instable because of occurrence of poles in right-side of s-domain, and this may lead to realization complications. Due to practical design concerns, we addressed a generic type of OBILI controller for the closed-loop control of a class of fractional order minimum phase plant models with n-fractional order denominator elements. This generic fractional-order controller structure allows matching with frequency response characteristics of Bode's ideal loops and possesses all frequency domain properties of Bode's ideal loop reference model. Furthermore, the optimal Bode's ideal loop reference model also makes an important practical contribution to optimal and robust loop shaping controller design methodologies. Essentially, the OBILI control design scheme reduces the need for solving optimization problems for optimal tuning of controller coefficients. Rather, the OBILI control design scheme can provide very effective generic fractional order controller solutions, particularly for minimum phase processes. To demonstrate these design improvements, the OBILI controller design scheme was illustrated for the closed-loop control of the fractional order heat furnace system model, and control performance improvements in terms of the ISE optimality and the robustness against parametric perturbation were verified by using Monte Carlo simulation for statistical analyses of performance robustness. Future works can address OBILI controllers for the non-minimum phase plant model and their realization problems.

Conflict of Interest

No conflict of interest was declared by the authors.

References

Alagoz, B.B., 2018. Fractional order linear time invariant system stabilization by brute-force search. Transactions of the Institute of Measurement and Control, 40(5), 1447–1456.

Alagoz, B.B., Ates, A., Yeroglu, C., 2013. Auto-tuning of PID controller according to fractional-order reference model approximation for DC rotor control. Mechatronics, 23(7), 789–797.

Arya, P.P., Chakrabarty, S., 2018. IMC based fractional order controller design for specific non-minimum phase systems. IFAC-PapersOnLine, 51(4), 847–852.

Åström, K.J.,2000. Limitations on control system performance. European Journal of Control, 6(1), 2–20.

Barbosa, R.S., Machado, T.J.A., Ferreire, I.M., 2004. PID controller tuning using fractional calculus concepts. Fractional Calculus and Applied Analysis, 7, 121–134.

Barbosa, R.S., Machado, J.A.T., Ferreira, I.M., 2004. Tuning of PID controllers based on bode's ideal transfer function. Nonlinear Dynamics, 38(1–4), 305–321.

Bode, H.W., 1945. Network analysis and feedback amplifier design. D. Van Nostrand Company.

Bolton, W., 2004. Frequency response. Instrumentation and Control Systems, pp. 252–281. Elsevier Science & Technology Books.

Bower, J.L., Schultheiss, P.M., 1961. Introduction to the design of servomechanisms. Wiley.

Chakraborty, S., Naskar, A.K., Ghosh, S., 2020. Inverse plant model and frequency loop shaping-based PID controller design for processes with time-delay. International Journal of Automation and Control, 14(4), 399–422.

Chen, Y., Moore, K.L., Vinagre, B.M., Podlubny, I., 2005. Robust PID Controller Autotuning With An Iso-Damping Property Through A Phase Shaper. Fractional Differentiation and its Applications,pp. 687–706.

Chen, Y.Q., Dou, H., Vinagre, B.M., Monje, C.A., 2006. A robust tuning method for fractional order PI controllers. IFAC Proceedings Volumes (IFAC-PapersOnline), 2(PART 1), 22–27.

Cho, J.-H., Hwang, H.-S., 2007. Design of PID Controller to Ensure Specified Phase Margin and Iso-damping Property Using Reduction Model. In: The Korean Institute of Electrical Engineers (KIEE) Conference, pp. 113–118.

Cho, J., Principe, J.C., Erdogmus, D., Motter, M.A., 2006. Modeling and inverse controller design for an unmanned aerial vehicle based on the self-organizing map. IEEE Transactions on Neural Networks, 17(2), 445–460.

Deniz, F. N., 2022. An effective Smith predictor based fractional-order PID controller design methodology for preservation of design optimality and robust control performance in practice. International Journal of Systems Science, 53(14), 2948–2966.

Doğruer, T., Yüce, A., Tan, N., 2017. PID Controller Design for a Fractional Order System using Bode's Ideal Transfer Function. Uluslararası Muhendislik Arastirma ve Gelistirme Dergisi, 9(3), 126–135.

Doyle, J., Francis, B., Tannenbaum, A.,1990. Feedback Control Theory. Macmillan.

Faisal, S.F., Beig, A.R., Thomas, S., 2021. Real-time implementation of robust loop-shaping controller for a vsc hvdc system. Energies, 14(16), 4955.

Feliu-Batlle, V., Castillo-García, F.J., 2014. On the robust control of stable minimum phase plants with large uncertainty in a time constant. A fractional-order control approach. Automatica, 50(1), 218–224.

Fergani, N., 2022. Direct synthesis-based fractional-order PID controller design: application to AVR system. International Journal of Dynamics and Control, 10(6), 2124–2138.

Horowitz, I.M., 1963. Synthesis of Feedback Systems. Academic Press.

Jeng, J.-C., Lin, S.-W., 2012. Robust proportional-integral-derivative controller design for stable/integrating processes with inverse response and time delay. Industrial & Engineering Chemistry Research, 51(6), 2652–2665.

Kealy, T., O'dwyer, A., 2003. Analytical ISE calculation and optimum control system design. In: Proceedings of the Irish Signals and Systems Conference, pp. 418–423.

Kharrazi, S., Lidberg, M., Fredriksson, J., 2012. A generic controller for improving lateral performance of heavy vehicle combinations. Proceedings of the Institution of Mechanical Engineers, Part D: Journal of Automobile Engineering, 227(5), 619–642.

Kumbasar, T., Eksin, İ., Guzelkaya, M., Yesil, E., 2011. Adaptive fuzzy model based inverse controller design using BB-BC optimization algorithm. Expert Systems with Applications, 38(10), 12356–12364.

Lanusse, P., Malti, R., Melchior, P., 2013. CRONE control system design toolbox for the control engineering community: Tutorial and case study. Philosophical Transactions of the Royal Society A: Mathematical, Physical and Engineering Sciences, 371(1990), 1–14.

Lee, P. L., Sullivan, G. R., 1988. Generic model control-theory and applications. IFAC Proceedings Volumes (IFAC-PapersOnline), 21(4), 111–119.

Li, H., & Chen, Y., 2008. A fractional order proportional and derivative (FOPD) controller tuning algorithm. In: Chinese Control and Decision Conference, pp. 4059–4063.

Li, H., Zhao, Y., Zhang, X., Zhang, B., Li, Z., 2020. An analytical parameter tuning method for fractional order PIλ controller based on ideal closed loop response. Developments of Artificial Intelligence Technologies in Computation and Robotics, In: Proceedings of the 14th International FLINS Conference (FLINS 2020), pp. 1391–1399.

Luo, Y., Chen, Y.Q., 2009. Fractional order [proportional derivative] controller for a class of fractional order systems. Automatica, 45(10), 2446–2450.

Manabe, S., 1960. The non-integer integral and its application to control systems. The Journal of The Institute of Electrical Engineers of Japan, 80(860), 589–597.

Matušů, R., Şenol, B., Pekař, L., 2018. Robust stability of fractional-order linear time-invariant systems: Parametric versus Unstructured Uncertainty Models. Complexity, 2018, 1–12.
Merrikh-Bayat, F., 2012. General rules for optimal tuning the PIλDμ controllers with application to first-order plus time delay processes. Canadian Society for Chemical Engineering, 90(6), 1400–1410.
Nagarsheth, S.H., Sharma, S.N., 2020. Control of non-minimum phase systems with dead time: a fractional system viewpoint. International Journal of Systems Science, 51(11), 1905–1928.
Narendra, K.S., Parthasarathy, K., 1990. Identification and control of dynamical systems using neural networks. IEEE Transactions on Neural Networks, 1(1), 4–27.
Podlubny, I., 1994. Fractional-order systems and fractional-order controllers. Slovak Academy of Science Institute of Experimental Physics: Vol. UEF-03-94.
Saha, S., Das, S., Ghosh, R., Goswami, B., Balasubramanian, R., Chandra, A.K., Das, S., Gupta, A., 2010. Design of a fractional order phase shaper for iso-damped control of a PHWR under step-back condition. IEEE Transactions on Nuclear Science, 57(3 PART 3), 1602–1612.
Sahoo, A.K., Mishra, S.K., 2021. Design of Lagrangian-based FOPID controller for desired closed loop system. Journal of Circuits, Systems and Computers, 30(04), 2150064.
Saidi, B., Amairi, M., Najar, S., Aoun, M., 2015. Bode shaping-based design methods of a fractional order PID controller for uncertain systems. Nonlinear Dynamics, 80(4), 1817–1838.
Saxena, S., Biradar, S., 2022. Fractional-order IMC controller for high-order system using reduced-order modelling via Big-Bang, Big-Crunch optimisation. International Journal of Systems Science, 53(1), 168–181.
Saxena, S., Hote, Y.V., 2022. Design of robust fractional-order controller using the Bode ideal transfer function approach in IMC paradigm. Nonlinear Dynamics, 107, 983–1001.
Shafiq, M., 2005. Internal model control structure using adaptive inverse control strategy. ISA Transactions, 44(3), 353–362.
Vinagre, B.M., Chen, Y.Q., Petráš, I., 2003. Two direct Tustin discretization methods for fractional-order differentiator/integrator. Journal of the Franklin Institute, 340(5), 349–362.
Vu, T.N.L.,Lee, M., 2014. Smith predictor based fractional-order PI control for time-delay processes. Korean Journal of Chemical Engineering, 31, 1321–1329.
Wang, C.Y., Jin, Y.S., Chen, Y.Q., 2009. Auto-tuning of FOPI and FO[PI] controllers with iso-damping property. In: Proceedings of the IEEE Conference on Decision and Control, 01(435), pp. 7309–7314.
Xue, D., 2017. Fractional-order control systems. Fundamentals and numerical implementations. De Gruyter, pp. 372.
Yadav, M., Hirenkumar, G.P., 2022. Control of non-minimum phase system using inverse response compensator with different approximations. International Journal of Modelling, Identification and Control, 40(1), 59–69.
Yumuk, E., Guzelkaya, M., Eksin, İ., 2016. Reduced integer order inverse controller design for single fractional pole model. In: 24th Mediterranean Conference on Control and Automation (MED), pp. 148–153.
Yumuk, E., Güzelkaya, M., Eksin, İ., 2019. Analytical fractional PID controller design based on Bode's ideal transfer function plus time delay. ISA Transactions, 91, 196–206.
Zhang, L., Zhang, Q., Wang, W., 2020. Application of Ideal Bode Transfer Function Tuning Fractional Order PID in Pressure Difference of Vertical Mill. In: Proceedings of the 32nd Chinese Control and Decision Conference, CCDC 2020, pp. 3501–3505.
Zhao, C., Xue, D., Chen, Y., 2005. A fractional order PID tuning algorithm for a class of fractional order plants. In: IEEE International Conference Mechatronics and Automation, pp. 216–221.
Zheng, W., Luo, Y., Chen, Y.Q., 2020. A fractional order controller design based on bode's ideal transfer function and bode's ideal cut-off ideas. IFAC-PapersOnLine, 53(2), 3663–3668.
Zhou, K., Doyle, J.C., Glover, K., 1998. Robust Optimal Control. Prentice Hall.
Zhuo-Yun, N., Yi-Min, Z., Qing-Guo, W., Rui-Juan, L., Lei-Jun, X., 2020. Fractional-Order PID Controller Design for Time-Delay Systems Based on Modified Bode's Ideal Transfer Function. IEEE Access, 8, 103500–103510.

Appendix:

A Matlab code for the numerical calculation of Eqn. 11 is given below.

```
% Matlab code for the numerical calculation of Eqn. 11
wc=100; % Crossover frequency
alpha=1; % Fractional order
% Matlab codes for Eq.11
fw=@(w,wc,alpha) (abs((1./(1+(wc./(sqrt(-1).*w)).^alpha)).*(1./(sqrt(-1).*w))).^2);
% Numerical integral calculation
E=(1/(2*pi))*integral(@(w) fw(w,wc,alpha),-1e+10,1e+10)
```